

Geometric Disentanglement by Random Convex Polytopes

Michael Joswig

Technische Universität Berlin, Chair of Discrete Mathematics/Geometry
MPI MiS Leipzig
joswig@math.tu-berlin.de

Marek Kaluba

Technische Universität Berlin, Chair of Discrete Mathematics/Geometry
Adam Mickiewicz University, Poznań, Poland
kaluba@math.tu-berlin.de

Lukas Ruff

Technische Universität Berlin, Dept. of Electrical Engineering and Computer Science
lukas.ruff@tu-berlin.de

Abstract

We propose a new geometric method for measuring the quality of representations obtained from deep learning. Our approach, called *Random Polytope Descriptor*, provides an efficient description of data points based on the construction of random convex polytopes. We demonstrate the use of our technique by qualitatively comparing the behavior of classic and regularized autoencoders. This reveals that applying regularization to autoencoder networks may decrease the out-of-distribution detection performance in latent space. While our technique is similar in spirit to k -means clustering, we achieve significantly better false positive/negative balance in clustering tasks on autoencoded datasets.

1 Introduction

Finding meaningful data representations that capture the information relevant for some task lies at the very core of any data-driven discipline such as statistics or machine learning. In contrast to handcrafted data features, representation learning [5] aims to *learn* such representations from the data itself. The concept of representation learning is fundamental to deep learning [39, 59], which has set the state of the art in recent years in numerous domains such as computer vision, speech recognition, or natural language processing. Deep representation functions are given by multi-layered neural networks that are parameterized by weights which are jointly optimized on some learning objective.

Despite the ubiquitous success of (supervised or unsupervised) representation learning for grouping given data into clusters and classes, the existing methods are still lacking, sometimes dramatically. To understand the problem, let us consider an example. Standard methods for dimensionality reduction include autoencoder networks. If the network faithfully represents the data, the clusters should be well separated in the latent space. Our first goal is to find tools for validating this hypothesis. Secondly, for a typical application we want to reduce the false positive rate resulting from misclassification. For example, falsely classifying out-of-distribution (OOD) samples into the classes of the training data in-distribution.

What makes a representation meaningful and which general principles are useful for representation learning is being actively discussed [5, 18, 66, 41, 67]. One prominent line of research considers the statistical nature of disentanglement [58, 4, 5, 14, 35, 41, 42], which is rooted in the idea that a learned representation should “separate the distinct, informative factors of variation in the data” [41]. While this is a valuable notion, other important properties of representation learning such as smoothness, the hierarchy of concepts, temporal and spatial coherence, or the preservation of natural clusters are also desired [5] and have been less studied. In this work, we focus on the convexity of classes and clusters in the image of deep neural networks to provide a geometric perspective on representation learning.

Convexity is a natural and fundamental representation property in machine learning in general. For instance, the separation of classes via multiple hyperplanes or half-spaces in supervised classification, such as for Support Vector Machines (SVMs) [60] in the Reproducing Kernel Hilbert Space via the hinge loss or for deep neural networks [22] in the output space via the cross-entropy loss, forms polyhedra that are convex and generally unbounded. Moreover, many well-known unsupervised learning methods make explicit convexity assumptions on the support of the data representation, such as Voronoi cells in k -means clustering or ellipsoids in Gaussian Mixture Models. Yet, it is worth noting that convexity is also implicit in Gaussian prior assumptions in popular deep generative models such as Variational Autoencoders (VAEs) [31, 53, 66], Generative Adversarial Networks [21, 16, 17], or Normalizing Flows [52, 32, 30]. Finally, one-class classification methods for support estimation such as the One-Class SVM [61] or (Deep) Support Vector Data Description [65, 55] also rely on convexity assumptions on the data representation via maximum-margin hyperplane or minimum enclosing hypersphere descriptions, respectively.

In this work, we propose a scalable and robust method called *Random Polytope Descriptor* (RPD) for evaluating convexity in representation learning. Our method is based on concepts from convex geometry and constructs a polytope (a piecewise-linear, bounded convex body) around the training data in representation space. Since polytopes by themselves may also suffer from a combinatorial explosion, we construct our descriptor from random convex polytopes instead which also makes it more robust. Finally, using the proximities to such polytopes allows us to judge the *geometric disentanglement* of representations, i.e., how well classes and clusters are separated into convex bodies. Our main contributions are the following:

- We propose the RPD method which is based on the construction of random convex polytopes for evaluating convexity in representation learning.
- We derive RPD from geometric principles and demonstrate its scalability.
- In experiments on autoencoder representations, we observe that RPD significantly reduces the false positive rates for out-of-distribution samples over k -means clustering and find that popular autoencoder regularization variants such as VAEs can destroy geometric information that is relevant for out-of-distribution detection.

2 Related Work

How to evaluate the quality and usefulness of a representation is a difficult question to answer in general and subject of ongoing research [5, 18, 66, 41, 67]. If only a single task is of interest, a straightforward approach would be to evaluate the performance of a representation on some measure that is meaningful to this task. Considering supervised classification, for instance, one might evaluate the quality of a model and representation by using the accuracy measure, i.e., by how well the representation separates some test data via hyperplanes in agreement with the respective ground-truth labels. However, even on standard tasks such as classification, other representation properties such as the robustness towards out-of-distribution samples [48, 23, 36, 40, 55] and adversarial attacks [63, 11, 6, 12], or model interpretability and decision explanation [44, 37, 56] might be desirable and thus

relevant representation quality criteria. This matter becomes even more challenging in the unsupervised or self-supervised setting, where the goal is to learn more generic data representations that prove useful for a variety of downstream tasks (e.g., multi-task or transfer learning) [69, 54, 64].

Bengio et al. [5] have collected and formulated some well-known generic criteria for representation learning, or *generic priors*. These include smoothness, the hierarchy of concepts (e.g., for images going from low-level pixel to high-level object features), semi-supervised learning (representations for supervised and unsupervised tasks should align), temporal and spatial coherence (small variations across time and space should result in similar representations), the preservation of natural clusters (data generated from one categorical variable should have similar representations), and statistical disentanglement (a representation should separate the distinct, informative factors of variation). Different variants of the Variational Autoencoder (VAE) [31, 53, 24, 35, 29, 13] which emphasize statistical disentanglement are currently considered as the state of the art for unsupervised representation learning [66, 41]. These approaches are closely related to earlier works on (non-linear) independent component analysis (ICA) which study the problem of recovering statistically independent (latent) components of a signal [15, 3, 25, 2, 28].

As mentioned above, the convexity of classes and natural clusters is a fundamental representation property that is often expressed only implicitly through model assumptions. The property that linear interpolations between data representations of one class/cluster should stay in the same class/cluster naturally ties into the generic priors above. This adheres to the simplicity principle from Bengio et al. [5]: “in good representations, the factors are related through simple, typically linear dependencies.”

3 Methods

We are interested in settings in which the data is composed of different unobserved groups (clusters or classes), and where the joint distribution of observed variables is a mixture of the group-specific distributions. This setting might be exemplified by assuming that the data come from a mixture of (latent) multivariate multinomial distributions, which is the natural assumption in many machine learning tasks such as clustering or classification. We further assume, that the super-level sets of the probability density function for each group-specific distribution in the mixture form a convex set, except maybe for regions of very low probability.

Our method is designed to work well on embeddings into feature space, where each of the classes are embedded into mutually disjoint convex sets. Such assumption is at the foundation of classical methods, for example SVMs, as mentioned above. These methods, however, by simply partitioning the whole feature space among classes, do not take the finiteness of training data into account, i.e., most classes are usually given infinite regions. While such a feature space might seem desirable, as it affords generalization properties for models under a closed set assumption (assuming that only K clusters or classes exist), it also increases the surface for adversarial and out-of-distribution attacks in open set situations [57]. Here we attempt to remedy this limitation by explicitly partitioning the feature space into compact convex regions and one unbounded (non-convex) “out-of-distribution” set.

Our basic idea is to use the convex hull $\text{conv}(X)$ of a set of points X from a given class and the distance to $\text{conv}(X)$ as a dissimilarity score. As mentioned earlier, both the convex hull computation and distance from a polytope are prohibitively expensive in high dimensions. Therefore, we will replace both of these steps with suitable approximations. In this section, we recall the *dual bounding bodies* of X and show how these polytopes can be modified into an efficient descriptor separating the points in the set X from the exterior. Instead of computing the actual distance, we will use the *scaling distance* (a piecewise-linear scaling of euclidean distance) from a certain *central point* of the polytope as a substitute.

3.1 An Idealized Setting

We consider K distinct sets $X_1, X_2, \dots, X_K \subset \mathbb{R}^d$, where X_k is the set of n_k samples of class k , seen in feature space \mathbb{R}^d . Associated with these classes are the K convex sets

$$\begin{aligned} P_k &= \text{conv}(X_k) \\ &= \left\{ \sum_{i=1}^{n_k} \lambda_i x_i \mid x_i \in X_k, 0 \leq \lambda_i, \sum \lambda_i = 1 \right\}. \end{aligned}$$

If all pairwise intersections $P_k \cap P_j$ are disjoint for $k \neq j$, then these convex sets provide perfect descriptors, if we have an oracle to test whether a new sample $x \in \mathbb{R}^d$ is contained in one of the sets P_1, P_2, \dots, P_K or their complement.

In the applications below each class X_k will be finite, whence the sets P_k form convex polytopes; see Ziegler [71] for general background, or Joswig and Theobald [27] for a more algorithmic view on the subject. Usually we will stick to finite sets and polytopes. In this case an oracle for checking $x \in P_k$ is given by linear programming. While linear programs can be solved in (weakly) polynomial time [62], they are still rather expensive in high dimensions; see Boyd and Vandenberghe [9] for a practical guide. If many samples need to be checked it is thus desirable to convert each set X_k into a description in terms of linear inequalities. A minimal encoding of this kind is given by the facets of the polytope P_k . Then, the containment $x \in P_k$ can be decided in $O(m_k d)$ time, where m_k is the number of facets of P_k . We assume that each set X_k affinely spans \mathbb{R}^d , whence P_k is full-dimensional, and thus its facet description is unique.

Converting X_k into the facets of $P_k = \text{conv}(X_k)$ is the *convex hull problem*. It is worth noting that the dual problem of computing the vertices of a polytope given in terms of finitely many linear inequalities (assuming that it is bounded) is equivalent to the convex hull problem by means of cone polarity. Letting n_k be the cardinality of X_k , McMullen's upper bound theorem [43] says that

$$m_k \in O\left(n_k^{\lfloor d/2 \rfloor}\right), \quad \text{if } d \text{ is considered constant.} \quad (1)$$

That bound is actually tight as can be seen, for example, from cyclic polytopes. In view of cone polarity, the same (tight) estimate holds for the number of vertices if the number of inequalities is given. This means that the number of vertices and the number of facets of a polytope may differ by several orders of magnitude.

The above sketch of a classification algorithm is too naive to be useful in practice. Yet, it is instructive to keep this in mind as a guiding principle. We identify three issues:

1. The idealized setup does not deal with outliers, i.e. is generally not robust.
2. Computing the convex hull of each class can be prohibitively expensive.
3. The K classes may not be well represented by their convex hulls.

Our main algorithmic contribution is a concept for addressing all three issues simultaneously. For empirical data on convex hull computation see Assarf et al. [1].

3.2 Dual Bounding Bodies

A first key idea is to replace convex hulls by suitable dual bounding bodies, which form outer approximations. To explain the concept it suffices to consider a single class. Let \mathbb{S}^{d-1} denote the $(d-1)$ -dimensional sphere of unit vectors in \mathbb{R}^d . Let $X \subset \mathbb{R}^d$, and suppose that $Y \subset \mathbb{S}^{d-1}$ is finite.

Definition 1. The **dual bounding body** of X with respect to Y is the polyhedron

$$D_Y(X) = \left\{ v \in \mathbb{R}^d \mid \langle v, y \rangle \leq \sup_{x \in X} \langle x, y \rangle \text{ for } y \in Y \right\}. \quad (2)$$

By construction $D_Y(X)$ is convex, and it contains X ; so it also contains $P = \text{conv}(X)$. If X is finite, then the supremum in (2) is a maximum attained for some $x \in X$, which only depends on y . In that case $D_Y(X) = P$ if and only if for each facet of P the set Y contains a normal vector of that facet. Checking if $x \in \mathbb{R}^d$ is contained in $D_Y(X)$ takes $O(|Y|d)$ time. In our analysis the sets X and Y will receive different roles; for a simple terminology we call the elements of X *points* and the elements of Y *directions*.

In the sequel we will assume that both, X and Y , are finite, and that Y is *positively spanning*, i.e., $\text{conv}(Y)$ contains the origin in its interior. As X is finite, the latter property is satisfied if and only if the polyhedron $D_Y(X)$ is bounded (i.e., is a polytope).

3.3 Random Polytope Descriptors

We propose a certain class of convex polytopes as approximate descriptions of learned representations in \mathbb{R}^d . Their algorithmic efficiency and robustness to the presence of outliers can be controlled by a pair of hyperparameters. Again we assume that $X \subset \mathbb{R}^d$ is finite with $n = |X|$.

Definition 2. Let $Y \subset \mathbb{S}^{d-1}$ be a set of m directions chosen uniformly at random, and let ℓ be a positive integer. The **Random Polytope Descriptor** (RPD) is the polyhedron

$$\text{RPD}_{m,\ell}(X) := \{v \in \mathbb{R}^d \mid \langle v, y \rangle \leq \ell\text{-max}_{x \in X} \langle x, y \rangle, y \in Y\} , \quad (3)$$

where ℓ -max denotes the ℓ -th largest scalar product.

Tacitly we will assume that $\text{RPD}_{m,\ell}(X)$ is bounded. This is the case if and only if Y is positively spanning. The random polytope descriptors form a variation of the dual bounding bodies; more precisely, $\text{RPD}_{m,1}(X) = D_Y(X)$.

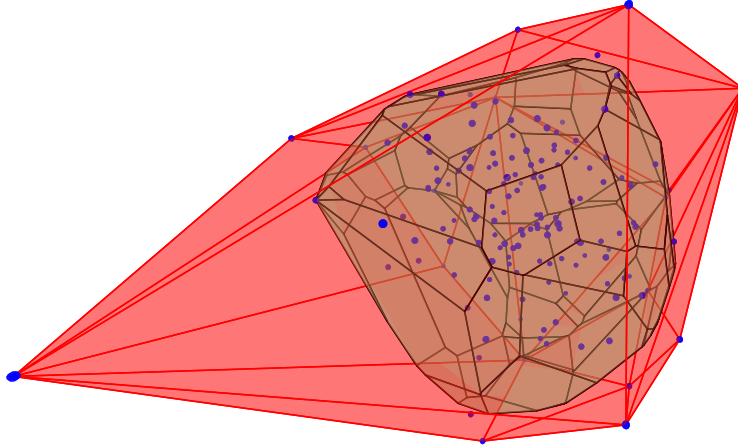


Figure 1: Convex hull $\text{conv}(X)$ (red) and random polytope descriptor $\text{RPD}_{80,3}(X)$ (green). Here $d = 3$, and $X \sim N(0, I)$ is a random Gaussian sample of 150 points with mean 0 and identity covariance I . Despite 3% outliers, the descriptor closely approximates the convex hull of the normal class (i.e., the inner cluster).

We briefly explain what it means to compute $\text{RPD}_{m,\ell}(X)$, and which cost this incurs. First we need m random unit vectors, which can be found in $O(m)$; see Knuth [33], §3.4.1.E.6. There is no reason to be overly exact here, so it is adequate to assume that the coefficients of the random vectors are constantly bounded. Consequently, all our complexity estimates are expressed in the unit cost model. Throughout, we take the feature space dimension d as a constant. Given X , we then evaluate mn scalar products to obtain a description in terms of

inequalities (so called H-representation) (3) of $\text{RPD}_{m,\ell}(X)$, resulting in a total complexity of $O(mn)$.

In the context of unsupervised anomaly detection (see Section 4.3) it is often beneficial to discard a fixed amount of data from X , i.e., label them as anomalous. The ℓ -max function serves as a “threshold” to eliminate the most extreme points from the training set. For (semi-)supervised learning, we note there may be natural candidate functions to replace ℓ -max to define variants of RPD, e.g., based on density estimation, weights, the value of a random variable, or simply the label. However, in this work, we focus on the unsupervised setting.

3.4 Scaling Distance and Anomaly Score

Let $P \subset \mathbb{R}^d$ be a full-dimensional convex polytope with a *central point* c . We only require that c is some fixed point in the interior of P . The *scaling distance* of $x \in \mathbb{R}^d$ to P with respect to c is defined as

$$\text{sd}_c(x, P) := \min \{ \alpha \geq 0 \mid x \in \alpha(P - c) + c \} . \quad (4)$$

This is the smallest number $\alpha \geq 0$ such that P inflated by a factor of α from the *central point* c contains x . The point x is contained in P if and only if $\text{sd}_c(x, P) \leq 1$.

If P is an RPD (as in Definition 2), the scaling distance can serve as a dissimilarity (anomaly) score, where the points further away from P are assigned higher scores. Given x , c , and an H-representation of P in terms of m linear inequalities, we can compute $\text{sd}_c(x, P)$ in $O(m)$ time, for d constant, by evaluating just scalar products.

There are several natural candidates for the central point c of a polytope P , which differ with respect to computational complexity, when P is given in terms of inequalities. For instance, the *centroid* is the center of gravity of P ; this is hard even to approximate, see Rademacher [49]. The *vertex barycenter* is the average of the vertices of P ; this is hard to compute exactly, see Elbassioni and Tiwary [20]; further results in loc. cit. make it unlikely that there is an efficient approximation procedure either. The *Chebyshev central point* is the center of the largest *sphere inscribed* to P ; this can be computed in $O(\sqrt{m})$ time by linear programming; see Eaves and Freund [19] and Renegar [51]. Note that the latter worst case complexity assumes that the bit representation of each inequality in the H-description of P is constantly bounded. For the special case of $P = \text{RPD}_{m,\ell}(X)$, where X is a normally distributed random sample, all three central points discussed are arbitrarily close to the origin, with high probability. We say that a property, depending on $m \in \mathbb{N}$, holds “with high probability” if it holds with probability converging to 1 as m approaches infinity.

A fourth candidate is the *sample mean*, which is the average over the given point set X . Notice, that it may happen that the sample mean is not contained in $P = \text{RPD}_{m,\ell}(X)$ for $\ell > 1$, i.e., if outliers have been discarded. Yet, in the normally distributed setting, the sample mean is also arbitrarily close to the origin, with high probability. In Section 4 we use the sample mean due to its simplicity and observed better performance in higher dimensions. However, Theorem 4 will provide an argument in favor of the vertex barycenter.

Let $X = \bigcup_k X_k$ be the training data partitioned into classes. For the *estimated distance* of a point $x \in \mathbb{R}^d$ to the combined support of all classes we take the minimum

$$\delta(x) := \min_k \{ \text{sd}_{c_k}(x, P_k) \} \quad (5)$$

of the scaling distances, where $P_k = \text{RPD}_{m,\ell}(X_k)$ and c_k is the respective central point. Note that $\delta(x)$ is a random variable as the construction of polytopes P_k is not deterministic. If the estimated distance to the combined support is larger than one, then evaluating (5) assigns a class which is closest to x , namely the index k at which the minimum is attained. For generic x this is unique. It follows from our complexity analysis above that estimating the distance to the combined support takes $O(m)$ time, for d and K fixed. This assumes that the central points c_1, \dots, c_K are known. For the sample means that cost is linear in the size of X .

3.5 Vertices and Their Barycenters

In this section we show that RPDs (as in Definition 2) are exceptionally benign from a computational point of view. This is of independent interest in view of ongoing research on random polytopes theory [10, 50, 47]. We make use of the *Rotation-Symmetry Model (RSM)* of Borgwardt [7] for random polytopes.

Theorem 3. *Let $X \sim N(0, I)$ either be normally distributed with mean zero (and identity covariance matrix). Or let X be uniformly distributed on the sphere \mathbb{S}^{d-1} . In both cases, for arbitrary m and ℓ , the number of vertices of $\text{RPD}_{m,\ell}(X)$ is of order $\Theta(m)$, with high probability, for d constant.*

Proof. The normal distribution and the uniform distribution are both rotationally invariant, and so is the uniform choice of directions $Y \subset \mathbb{S}^{d-1}$. Consequently, the construction of $\text{RPD}_{m,\ell}(X)$ follows the RSM, with m inequalities, and this yields the claim. \square

Theorem 3 says that RPDs have very few vertices, with high probability, in sharp contrast to the worst case scenario described by the upper bound theorem (1). More precisely, they form a *slender family* in the sense of Newman [47].

Next we want to discuss approximating the vertex barycenter of an RPD. This is meant to complement the discussion in Section 3.4. To keep the exposition concise we now focus on X is uniformly sampled from \mathbb{S}^{d-1} , which is the easiest RSM type; this leads to the random polytopes $P(d, n)$. We say that $P \sim P(d, n)$ if $P = \text{conv}(X)$, where $X \subset \mathbb{S}^{d-1}$ comprises n points chosen uniformly at random. With high probability, such a polytope is simplicial, it has n vertices, its $\Theta(n)$ many facets can be computed in $O(n^2)$ time, and the vertex barycenter lies arbitrarily close to the origin, for d constant [8]. Note that here $D_X(X)$ agrees with *polar dual* $P^\vee := \{v \in \mathbb{R}^d \mid \langle v, x \rangle \leq 1, x \in X\}$.

Theorem 4. *Let $P = \text{conv}(X) \sim P(d, n)$ as above. Further, let $Y \subset \mathbb{S}^{d-1}$ be a set of m directions chosen uniformly at random. Fix $\varepsilon > 0$ and $0 < p < 1$. Then the mean of s randomly chosen vertices of $D_Y(X)$ is at distance $\leq \varepsilon$ from the origin with probability at least $1 - p$ if*

$$s > \left(1 + \frac{2}{d} \log \left(\frac{2}{p} \right) \frac{e}{e-1} \cdot \frac{1}{\varepsilon^2(1-h_0)^2} \right) ,$$

where h_0 is the Hausdorff distance of P to the sphere \mathbb{S}^{d-1} .

Proof. The condition $d_H(P, \mathbb{S}^{d-1}) \leq h$, where d_H is the Hausdorff distance, may be read as: the height of the largest spherical cap cut from \mathbb{S}^{d-1} by some facet of P is at most h . So we have

$$d_H(D_Y(X), \mathbb{S}^{d-1}) \leq h(d, m, p) ,$$

with probability $1 - p$, where $h(d, m, p)$ is the distance resulting from the worst case scenario of all points from Y missing the largest spherical cap induced by P . Formally,

$$h(d, m, p) := \inf \left\{ h \mid \binom{m}{d} (1 - \text{NCA}_d(h))^{m-d} \leq \frac{p}{2} \right\} ,$$

where, $\text{NCA}_d(h)$ is the area of a spherical cap of height h normalized so that $\text{NCA}_d(1) = 1$ regardless of dimension. Note that all facets of $D_Y(X)$ are contained in a $(1, 1+h)$ d -dimensional annulus around the origin. Now the claim follows from Newman [47], Lemma 21. \square

Now let X be uniformly distributed on the translated sphere $v + \mathbb{S}^{d-1}$. Then the vertex barycenter of $D_Y(X)$ is close to v , with high probability. The following result says that v can be recovered from $D_Y(X)$ quickly, and the running time does not depend on the cardinality of X .

Corollary 5. *Let $D_Y(X)$ be given in terms of m linear inequalities. Then its vertex barycenter can be approximated, with high probability, in $O(\sqrt{m})$ time.*

Proof. By Theorem 4 it suffices to know a constant number of random vertices of $D_Y(X)$ to approximate the vertex barycenter, for given ε and p . Solving a linear program, with the m inequalities describing $D_Y(X)$ as constraints and a random direction as the objective function, provides one random vertex. Each such linear program can be solved in $O(\sqrt{m})$ [51]. \square

Standard results on the RSM [7] suggest that a version of Corollary 5 also holds for X normally distributed with v as its unknown mean, and for $\text{RPD}_{m,\ell}(X)$ instead of $D_Y(X)$, albeit at a slightly higher cost. The somewhat technical details are beyond our current scope.

3.6 Convex Separation

Since we do not use any a priori knowledge on the latent representation that we work with, it may happen that the RPDs of two (or more) classes intersect nontrivially. Again let $X = \bigcup_k X_k$ be partitioned into classes and $P_k = \text{RPD}_{m,\ell}(X_k)$ are the RPDs, for some fixed values of m and ℓ . Then we can define the *confusion coefficient* of classes k and j as

$$\gamma_{kj} := \frac{|\{X_k \cap P_j\}| + |\{X_j \cap P_k\}|}{|X_k \cup X_j|}, \quad (6)$$

i.e., a low value indicates good separation. This may be seen as a Monte Carlo style approximation of the integral of the probability density function of the data over the intersection $P_k \cap P_j$. Again by evaluating scalar products, computing one confusion coefficient is in $O(mn)$.

4 Experiments

We are interested in understanding better the geometry of feature spaces learned by deep autoencoders. In the following experiments, we compare and use RPD as a quality measure to examine and validate the convexity assumption in the latent space of established deep autoencoder models.

4.1 Experimental Setup

Datasets In our experiments we use the known MNIST [38], Fashion-MNIST (FMNIST) [70], and CIFAR-10 [34] image datasets, each containing $K = 10$ classes. Additionally, we consider the SVHN dataset [46] as out-of-distribution data in one of our evaluations.

Autoencoders We train standard (“bottleneck”) AE and VAE models on MNIST, FMNIST, and CIFAR-10 (for 5 seeds each) to embed the datasets into d -dimensional latent feature spaces for various choices of d . We use LeNet-type architectures for the encoders with two (three) 5×5 convolutional layers and max-pooling for MNIST and FMNIST (CIFAR-10), followed by two fully connected layers that map to the encoding of dimensionality d . We construct the corresponding decoders symmetrically, where we replace convolution and max-pooling with deconvolution and upsampling respectively. We apply leaky ReLU activations and batch normalization [26]. For training, we always take the entire training datasets, minimizing the reconstruction error (AE) and the reconstruction error regularized by a Gaussian prior on the latent distribution (VAE). Note that none of the networks are given any explicit convexity prior (apart from the Gaussian prior for VAE).

Table 1: AUC scores of $\text{RPD}_{640,1}$ and k -means for AE and VAE models trained on MNIST (classes 0–9 in (a)) and FMNIST (classes $F0$ – $F9$ in (b)) with embedding dimensionality $d = 16$. We set $\ell = 1$ in this experiment, as the RPDs are trained in a supervised setting, and thus no pollution of the training data is expected. Justification for choosing $m = 640$ is given in sensitivity analysis in Section 4.3.

(a) MNIST					(b) FMNIST				
Class	AE		VAE		Class	AE		VAE	
	RPD	k -means	RPD	k -means		RPD	k -means	RPD	k -means
0	99.6	99.3	99.2	96.1	$F0$	91.2	93.9	94.7	94.3
1	99.8	99.5	99.8	98.6	$F1$	98.3	99.0	98.9	98.1
2	94.6	94.0	96.3	93.4	$F2$	90.1	90.6	89.9	87.8
3	95.8	95.9	96.2	95.5	$F3$	94.9	93.8	96.7	93.4
4	95.4	92.3	98.0	94.3	$F4$	91.0	90.9	92.5	90.5
5	93.4	88.8	96.0	90.3	$F5$	93.2	91.0	96.5	93.8
6	98.3	94.4	99.4	95.8	$F6$	83.8	83.5	84.0	77.9
7	95.7	94.4	97.0	95.2	$F7$	98.4	98.3	98.3	98.4
8	96.6	94.0	96.4	92.4	$F8$	92.7	94.4	96.2	92.9
9	97.5	95.1	97.6	93.5	$F9$	98.6	98.3	97.7	97.8

4.2 Comparing RPD to k -means

We first compare RPD to a common k -means classifier which finds the mean of each class and then assigns a score to each sample based on the distance to the class mean. The resulting classifier, in geometric terms, partitions the latent space into Voronoi regions of the class means; see Joswig and Theobald [27] for a discussion of Voronoi diagrams and algorithms. In contrast, the RPD classifier is based on the scaling distance to the class polytopes with respective sample means. We train the classifiers on the AE and VAE embeddings of the MNIST and FMNIST training sets, respectively, and evaluate the separation of each class on the full test sets using the common Area Under the ROC curve (AUROC or AUC) metric.

While RPD and k -means are similar in spirit, they have significant differences. Due to the non-isotropic nature of the scaling distance, RPD should achieve a tighter convex description than k -means, especially when clusters in feature space are not spherical (rotation invariant). This is true for VAE networks, for example, if the latent space dimension is too low as clusters become packed. Therefore, we expect RPD to have fewer false positives at the same false negative rates, or equivalently, RPD to achieve better AUCs in this experiment; see Table 1. From the reasonably high performance of RPD, we can conclude that the convexity assumption is mostly satisfied for these networks.

Another key advantage of RPDs are the canonical rejection thresholds given by the scaling distance, which can be understood as assigning another “unknown” class to low density areas in the latent space. A threshold to replicate such behavior for k -means classifier would need to be found a posteriori (e.g., must be learned), but this increases the complexity and may result in a bias.

We note that constructing the H-representation (3) of the RPD is very fast in practice. On modern hardware¹, it takes less than 3s to create an $\text{RPD}_{640,2}(X)$ from a set X of 6000 points in \mathbb{R}^{20} , with respect to the Chebyshev central point. That time drops well under 1s if the sample mean is used as the central point instead. Evaluating the scaling distance (4)

¹Timings given for Intel i5-6200U processor.

takes less than 0.001s per sample in this scenario.

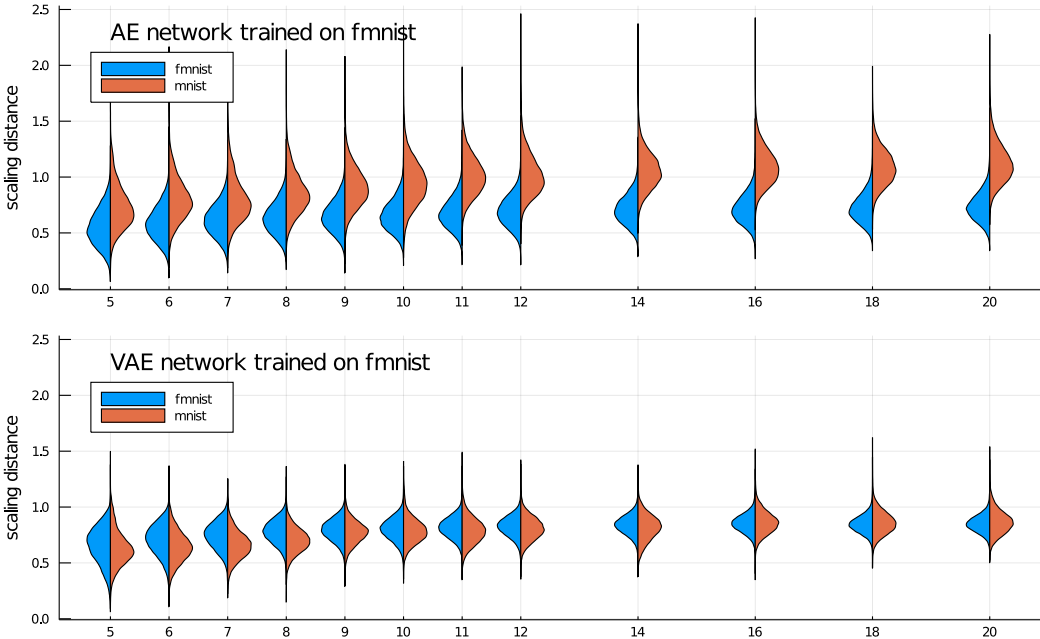


Figure 2: Results of the out-of-distribution detection experiment. AE and VAE networks were trained on FMNIST data and used to embed MNIST test sets. The plot depicts the distribution of minimal scaling distance to one of the ten FMNIST random polytope descriptors in various dimensions up to 20 for fixed $(m, \ell) = (640, 1)$. Five distinct AE and VAE networks were trained and independently five random polytopes were drawn for each of the dimensions.

4.3 Sensitivity Analysis of RPD in Anomaly Detection

We create an unsupervised anomaly detection scenario for each class of the MNIST and FMNIST datasets and measure the class separation into convex clusters in latent space. The training data X'_k contains all training data points from class k (normal samples) contaminated with $p|X_k|$ data points chosen uniformly at random from the respective other classes (anomalies) for some $0 < p < 1$. We then train a descriptor $P_k = \text{RPD}_{m,\ell}(X'_k)$ on this contaminated data and evaluate the separation (anomaly detection) performance again on the entire test set using AUC. This experiment may also be seen as a stochastic approximation of the intersection $P_k \cap \bigcup_{j \neq k} P_j$. Indeed, if there is an intersection of two RPDs on the test set, the points in the intersection are false negatives in the anomaly detection task.

Additionally, we perform a sensitivity analysis of the RPD hyperparameters ℓ and m . To assess the dependence on these parameters, we evaluate the performance for the following choices: $p = 0.02$, $\ell = 2$, and a grid of parameters (m, d) in the range $160 \leq m \leq 1280$ and $d \in \{5, \dots, 20\}$. As each MNIST and FMNIST class contains ~ 6000 training data points, we can expect ~ 120 outliers in the contaminated training set for a level $p = 0.02$. Based on this knowledge one may also choose ℓ (relating it to m) so that roughly the correct number of points is excluded when RPD is created. We provide the full results in Figs. 3 to 6 in the Appendix and only discuss the main findings here.

Comparison of AE and VAE Using RPD, we find that on MNIST the VAE representation seems to split the classes into fairly well-separated convex regions starting from $d = 9$ and

improving up to $d = 12$. For larger dimensions (and m fixed), the performance deteriorates slightly. This is expected in this case, as in higher dimensions a larger number of hyperplanes would be needed for a similar quality of approximation. On the more complex FMNIST dataset, we observe no deterioration in performance with growing dimension (Fig. 4). Overall VAE models seem to be superior to AE. The sustained high performance for VAE models on FMNIST might indicate that the intrinsic dimensionality of this dataset is higher than what has been studied here. On the practical side of network design, one may conclude that the regularization in VAE networks is too strong on MNIST.

Sensitivity Analysis When fixing the number of hyperplanes m , we see a monotonous increase of scores with the dimension of the latent space (Figs. 3 and 4). This is consistent with the fact that a higher latent dimension allows for a more faithful representation of the data. When fixing the dimension d , we see a dependence of the scores on the number of hyperplanes m defining an RPD_m . The scores increase monotonously with m both for MNIST (Fig. 5) and FMNIST (Fig. 6). This agrees with our intuition, as with more hyperplanes the RPDs tighten their approximation of the true convex hull. Setting $m > 40d$ does not seem to yield any additional performance improvements.

4.4 Out-of-Distribution Detection

In this experiment, we are interested in the representation of out-of-distribution data in the autoencoder feature spaces. We can consider RPDs as a model for the support of the individual class distributions in the training data (the in-distribution). Here we check how well this approximation works to detect out-of-distributions samples. We perform experiments with FMNIST (CIFAR-10) serving as the in-distribution (upon which the models are trained), and MNIST (SVHN) as the out-of-distribution dataset. This way, the arguably more complex datasets are used for training, while the simpler ones are only embedded for out-of-distribution investigation. This choice of datasets is motivated by the recent observation, that deep generative models can assign higher likelihood to (simpler) out-of-distribution datasets [45].

For each of the ten classes of the in-distribution training set X , we construct a random polytope $\text{RPD}_{m,1}(X_k)$. Since there is no contamination in this scenario, $\ell = 1$ is the natural choice. Based on our previous sensitivity analysis (see Section 4.3 and specifically Fig. 6) we choose $m = \max(640, 40d)$ as higher values of m showed little to no influence on performance. We then evaluate the estimated distance to the support (5) again on the respective test sets. The results are given in Fig. 2 and Fig. 7.

Comparison of AE and VAE The minimal scaling distances for FMNIST samples are well below 1 for both the AE and VAE models; recall from (4) that this signals containment in one of the classes. So this behavior is expected and an indicator for a reasonable performance of RPD for anomaly detection. However, we observe a clear distinction between the AE and VAE representation on the out-of-distribution samples (see Fig. 2). On the AE model trained on FMNIST, the MNIST out-of-distribution test data points have significantly higher dissimilarity score. In contrast, the VAE network embedding of MNIST test data exhibits almost complete overlap with the support of the FMNIST in-distribution. Hence, we conclude, that the VAE regularization destroys relevant information which may be exploited for out-of-distribution attacks. Note that we do not observe this distinction on CIFAR-10 vs. SVHN (see Fig. 7 in the Appendix), which might again be due to the intrinsic dimensionality of this data being higher than the highest case considered here ($d = 256$).

Finally, it is worth noting that for none of the examined test sets, the scores concentrate around 0. Instead they seem to be distributed near a sphere of some radius increasing with the dimension, similarly to the behavior of a Gaussian in high dimensions [68]. For the VAE models on FMNIST, for example, the mean and variance range from (0.68, 0.03) to (0.85, 0.006). This indicates that the analysis from Corollary 5 seems appropriate here.

5 Conclusion

We have introduced the Random Polytope Descriptor, a geometric method for measuring the convexity of classes. This has been derived from geometric principles, with theoretical arguments for its scalability. In our experiments with autoencoders we have shown that RPD significantly reduces the false positive rates for out-of-distribution samples over k -means. Further, we have found that autoencoder regularization variants (in particular VAEs) can destroy geometric information that is relevant for out-of-distribution detection.

In future work, it will be interesting to evaluate the robustness of RPD with respect to adversarial attacks, utilize RPD facets for interpreting deep representations, and use RPD to improve the explainability of deep feature spaces.

Acknowledgments

We thank Klaus-Robert Müller and Andrew Newman for fruitful discussions. MJ received partial support by Deutsche Forschungsgemeinschaft (EXC 2046: “MATH+”, SFB-TRR 195: “Symbolic Tools in Mathematics and their Application”, and GRK 2434: “Facets of Complexity”). MK was supported by Deutsche Forschungsgemeinschaft (EXC 2046: “MATH+”, Project EF1-3) and National Science Centre, Poland grant 2017/26/D/ST1/00103. LR acknowledges support by the German Federal Ministry of Education and Research (BMBF) in the project ALICE III (01IS18049B).

References

- [1] B. Assarf, E. Gawrilow, K. Herr, M. Joswig, B. Lorenz, A. Paffenholz, and T. Rehn. Computing convex hulls and counting integer points with `polymake`. *Math. Program. Comput.*, 9(1):1–38, 2017. doi: 10.1007/s12532-016-0104-z. URL <http://dx.doi.org/10.1007/s12532-016-0104-z>.
- [2] F. R. Bach and M. I. Jordan. Kernel independent component analysis. *Journal of Machine Learning Research*, 3(Jul):1–48, 2002.
- [3] A. J. Bell and T. J. Sejnowski. An information-maximization approach to blind separation and blind deconvolution. *Neural Computation*, 7(6):1129–1159, 1995.
- [4] Y. Bengio, Y. LeCun, et al. Scaling learning algorithms towards ai. *Large-Scale Kernel Machines*, 34(5):1–41, 2007.
- [5] Y. Bengio, A. Courville, and P. Vincent. Representation learning: A review and new perspectives. *IEEE Transactions on Pattern Analysis and Machine Intelligence*, 35(8):1798–1828, 2013.
- [6] B. Biggio and F. Roli. Wild patterns: Ten years after the rise of adversarial machine learning. *Pattern Recognition*, 84:317–331, 2018.
- [7] K.-H. Borgwardt. *The simplex method*, volume 1 of *Algorithms and Combinatorics*. Springer-Verlag, Berlin, 1987. ISBN 3-540-17096-0. doi: 10.1007/978-3-642-61578-8. URL <https://doi.org/10.1007/978-3-642-61578-8>. A probabilistic analysis.
- [8] K. H. Borgwardt. Average-case analysis of the double description method and the beneath-beyond algorithm. *Discrete Comput. Geom.*, 37(2):175–204, 2007. ISSN 0179-5376. doi: 10.1007/s00454-006-1257-8. URL <https://doi.org/10.1007/s00454-006-1257-8>.
- [9] S. P. Boyd and L. Vandenberghe. *Convex Optimization*. Cambridge University Press, 2004.

- [10] C. Buchta, J. Müller, and R. F. Tichy. Stochastic approximation of convex bodies. *Mathematische Annalen*, 271(2):225–235, Apr 1985. ISSN 1432-1807. doi: 10.1007/BF01455988. URL <https://doi.org/10.1007/BF01455988>.
- [11] N. Carlini and D. Wagner. Towards evaluating the robustness of neural networks. In *IEEE Symposium on Security and Privacy*, pages 39–57. IEEE, 2017.
- [12] N. Carlini, A. Athalye, N. Papernot, W. Brendel, J. Rauber, D. Tsipras, I. Goodfellow, A. Madry, and A. Kurakin. On evaluating adversarial robustness. *arXiv preprint arXiv:1902.06705*, 2019.
- [13] T. Q. Chen, X. Li, R. B. Grosse, and D. K. Duvenaud. Isolating sources of disentanglement in variational autoencoders. In *Advances in Neural Information Processing Systems*, pages 2610–2620, 2018.
- [14] X. Chen, Y. Duan, R. Houthooft, J. Schulman, I. Sutskever, and P. Abbeel. Infogan: Interpretable representation learning by information maximizing generative adversarial nets. In *Advances in Neural Information Processing Systems*, pages 2172–2180, 2016.
- [15] P. Comon. Independent component analysis, a new concept? *Signal processing*, 36(3): 287–314, 1994.
- [16] J. Donahue, P. Krähenbühl, and T. Darrell. Adversarial feature learning. In *International Conference on Learning Representations*, 2017.
- [17] V. Dumoulin, I. Belghazi, B. Poole, O. Mastropietro, A. Lamb, M. Arjovsky, and A. Courville. Adversarially learned inference. In *International Conference on Learning Representations*, 2017.
- [18] C. Eastwood and C. K. Williams. A framework for the quantitative evaluation of disentangled representations. In *International Conference on Learning Representations*, 2018.
- [19] B. C. Eaves and R. M. Freund. Optimal scaling of balls and polyhedra. *Math. Programming*, 23(2):138–147, 1982. ISSN 0025-5610. doi: 10.1007/BF01583784. URL <https://doi.org/10.1007/BF01583784>.
- [20] K. Elbassioni and H. R. Tiwary. Complexity of approximating the vertex centroid of a polyhedron. In *Algorithms and computation*, volume 5878 of *Lecture Notes in Comput. Sci.*, pages 413–422. Springer, Berlin, 2009. doi: 10.1007/978-3-642-10631-6_43. URL https://doi.org/10.1007/978-3-642-10631-6_43.
- [21] I. Goodfellow, J. Pouget-Abadie, M. Mirza, B. Xu, D. Warde-Farley, S. Ozair, A. Courville, and Y. Bengio. Generative adversarial nets. In *Advances in Neural Information Processing Systems*, pages 2672–2680, 2014.
- [22] I. Goodfellow, Y. Bengio, and A. Courville. *Deep Learning*. MIT press, 2016.
- [23] D. Hendrycks and K. Gimpel. A baseline for detecting misclassified and out-of-distribution examples in neural networks. In *International Conference on Learning Representations*, 2017.
- [24] I. Higgins, L. Matthey, A. Pal, C. Burgess, X. Glorot, M. Botvinick, S. Mohamed, and A. Lerchner. β -VAE: Learning basic visual concepts with a constrained variational framework. In *International Conference on Learning Representations*, 2017.
- [25] A. Hyvärinen and P. Pajunen. Nonlinear independent component analysis: Existence and uniqueness results. *Neural Networks*, 12(3):429–439, 1999.

- [26] S. Ioffe and C. Szegedy. Batch normalization: Accelerating deep network training by reducing internal covariate shift. In *International Conference on Machine Learning*, pages 448–456, 2015.
- [27] M. Joswig and T. Theobald. *Polyhedral and algebraic methods in computational geometry*. Universitext. Springer, London, 2013. ISBN 978-1-4471-4816-6. doi: 10.1007/978-1-4471-4817-3. URL <http://dx.doi.org/10.1007/978-1-4471-4817-3>. Revised and updated translation of the 2008 German original.
- [28] I. Khemakhem, D. P. Kingma, R. P. Monti, and A. Hyvärinen. Variational autoencoders and nonlinear ica: A unifying framework. In *International Conference on Artificial Intelligence and Statistics*, 2020.
- [29] H. Kim and A. Mnih. Disentangling by factorising. In *International Conference on Machine Learning*, pages 2649–2658, 2018.
- [30] D. P. Kingma and P. Dhariwal. Glow: Generative flow with invertible 1x1 convolutions. In *Advances in Neural Information Processing Systems*, pages 10215–10224, 2018.
- [31] D. P. Kingma and M. Welling. Auto-encoding variational bayes. In *International Conference on Learning Representations*, 2014.
- [32] D. P. Kingma, T. Salimans, R. Jozefowicz, X. Chen, I. Sutskever, and M. Welling. Improved variational inference with inverse autoregressive flow. In *Advances in Neural Information Processing Systems*, pages 4743–4751, 2016.
- [33] D. E. Knuth. *The art of computer programming. Vol. 2*. Addison-Wesley, Reading, MA, 1998. ISBN 0-201-89684-2. Seminumerical algorithms, Third edition [of MR0286318].
- [34] A. Krizhevsky and G. Hinton. Learning multiple layers of features from tiny images. Technical report, Citeseer, 2009.
- [35] A. Kumar, P. Sattigeri, and A. Balakrishnan. Variational inference of disentangled latent concepts from unlabeled observations. In *International Conference on Learning Representations*, 2017.
- [36] B. Lakshminarayanan, A. Pritzel, and C. Blundell. Simple and scalable predictive uncertainty estimation using deep ensembles. In *Advances in Neural Information Processing Systems*, pages 6402–6413, 2017.
- [37] S. Lapuschkin, S. Wäldchen, A. Binder, G. Montavon, W. Samek, and K.-R. Müller. Unmasking Clever Hans predictors and assessing what machines really learn. *Nature Communications*, 10:1096, 2019.
- [38] Y. LeCun, C. Cortes, and C. Burges. MNIST handwritten digit database, 2010.
- [39] Y. LeCun, Y. Bengio, and G. Hinton. Deep learning. *Nature*, 521(7553):436–444, 2015.
- [40] K. Lee, K. Lee, H. Lee, and J. Shin. A simple unified framework for detecting out-of-distribution samples and adversarial attacks. In *Advances in Neural Information Processing Systems*, pages 7167–7177, 2018.
- [41] F. Locatello, S. Bauer, M. Lucic, G. Raetsch, S. Gelly, B. Schölkopf, and O. Bachem. Challenging common assumptions in the unsupervised learning of disentangled representations. In *International Conference on Machine Learning*, pages 4114–4124, 2019.
- [42] E. Mathieu, T. Rainforth, N. Siddharth, and Y. W. Teh. Disentangling disentanglement in variational autoencoders. In *International Conference on Machine Learning*, pages 4402–4412, 2019.

- [43] P. McMullen. The maximum numbers of faces of a convex polytope. *Mathematika*, 17:179–184, 1970. ISSN 0025-5793. doi: 10.1112/S0025579300002850. URL <https://doi.org/10.1112/S0025579300002850>.
- [44] G. Montavon, W. Samek, and K.-R. Müller. Methods for interpreting and understanding deep neural networks. *Digital Signal Processing*, 73:1–15, 2018.
- [45] E. Nalisnick, A. Matsukawa, Y. W. Teh, D. Gorur, and B. Lakshminarayanan. Do deep generative models know what they don’t know? In *International Conference on Learning Representations*, 2019.
- [46] Y. Netzer, T. Wang, A. Coates, A. Bissacco, B. Wu, and A. Y. Ng. Reading digits in natural images with unsupervised feature learning. In *NIPS Workshop on Deep Learning and Unsupervised Feature Learning*, 2011.
- [47] A. Newman. Doubly random polytopes, 2020. Preprint [arXiv:2006.07000](https://arxiv.org/abs/2006.07000).
- [48] A. Nguyen, J. Yosinski, and J. Clune. Deep neural networks are easily fooled: High confidence predictions for unrecognizable images. In *Computer Vision and Pattern Recognition*, pages 427–436, 2015.
- [49] L. Rademacher. Approximating the centroid is hard. In *Computational geometry (SCG’07)*, pages 302–305. ACM, New York, 2007. doi: 10.1145/1247069.1247123. URL <https://doi.org/10.1145/1247069.1247123>.
- [50] M. Reitzner. Random polytopes. In *New perspectives in stochastic geometry*, pages 45–76. Oxford Univ. Press, Oxford, 2010.
- [51] J. Renegar. A polynomial-time algorithm, based on Newton’s method, for linear programming. *Math. Programming*, 40(1, (Ser. A)):59–93, 1988. ISSN 0025-5610. doi: 10.1007/BF01580724. URL <https://doi.org/10.1007/BF01580724>.
- [52] D. Rezende and S. Mohamed. Variational inference with normalizing flows. In *International Conference on Machine Learning*, pages 1530–1538, 2015.
- [53] D. J. Rezende, S. Mohamed, and D. Wierstra. Stochastic backpropagation and approximate inference in deep generative models. In *International Conference on Machine Learning*, volume 32, pages 1278–1286, 2014.
- [54] S. Ruder. An overview of multi-task learning in deep neural networks. *arXiv preprint arXiv:1706.05098*, 2017.
- [55] L. Ruff, R. A. Vandermeulen, N. Görnitz, L. Deecke, S. A. Siddiqui, A. Binder, E. Müller, and M. Kloft. Deep one-class classification. In *International Conference on Machine Learning*, volume 80, pages 4390–4399, 2018.
- [56] W. Samek, G. Montavon, S. Lapuschkin, C. J. Anders, and K.-R. Müller. Toward interpretable machine learning: Transparent deep neural networks and beyond. *arXiv preprint arXiv:2003.07631*, 2020.
- [57] W. J. Scheirer, A. de Rezende Rocha, A. Sapkota, and T. E. Boult. Toward open set recognition. *IEEE Transactions on Pattern Analysis and Machine Intelligence*, 35(7): 1757–1772, 2012.
- [58] J. Schmidhuber. Learning factorial codes by predictability minimization. *Neural Computation*, 4(6):863–879, 1992.
- [59] J. Schmidhuber. Deep learning in neural networks: An overview. *Neural Networks*, 61: 85–117, 2015.

- [60] B. Schölkopf and A. J. Smola. *Learning with Kernels*. MIT press, 2002.
- [61] B. Schölkopf, J. C. Platt, J. Shawe-Taylor, A. J. Smola, and R. C. Williamson. Estimating the support of a high-dimensional distribution. *Neural Computation*, 13(7):1443–1471, 2001.
- [62] A. Schrijver. *Theory of linear and integer programming*. Wiley-Interscience Series in Discrete Mathematics. John Wiley & Sons, Ltd., Chichester, 1986. ISBN 0-471-90854-1. A Wiley-Interscience Publication.
- [63] C. Szegedy, W. Zaremba, I. Sutskever, J. Bruna, D. Erhan, I. Goodfellow, and R. Fergus. Intriguing properties of neural networks. In *International Conference on Learning Representations*, 2014.
- [64] C. Tan, F. Sun, T. Kong, W. Zhang, C. Yang, and C. Liu. A survey on deep transfer learning. In *International Conference on Artificial Neural Networks*, pages 270–279. Springer, 2018.
- [65] D. M. Tax and R. P. Duin. Support vector data description. *Machine Learning*, 54(1): 45–66, 2004.
- [66] M. Tschannen, O. Bachem, and M. Lucic. Recent advances in autoencoder-based representation learning. In *3rd Workshop on Bayesian Deep Learning (NeurIPS 2018)*, 2018.
- [67] S. van Steenkiste, F. Locatello, J. Schmidhuber, and O. Bachem. Are disentangled representations helpful for abstract visual reasoning? In *Advances in Neural Information Processing Systems*, pages 14222–14235, 2019.
- [68] R. Vershynin. *High-Dimensional Probability: An Introduction with Applications in Data Science*, volume 47. Cambridge University Press, 2018.
- [69] K. Weiss, T. M. Khoshgoftaar, and D. Wang. A survey of transfer learning. *Journal of Big Data*, 3(1):9, 2016.
- [70] H. Xiao, K. Rasul, and R. Vollgraf. Fashion-MNIST: A novel image dataset for benchmarking machine learning algorithms. *arXiv preprint arXiv:1708.07747*, 2017.
- [71] G. M. Ziegler. *Lectures on polytopes*, volume 152 of *Graduate Texts in Mathematics*. Springer-Verlag, New York, 1995. ISBN 0-387-94365-X.

A Contracting Property of Autoencoders

Autoencoder networks can be seen as a pair of networks $\phi: \mathbb{R}^n \rightarrow \mathbb{R}^d$, $\psi: \mathbb{R}^d \rightarrow \mathbb{R}^n$ with

$$\psi \circ \phi: \mathbb{R}^n \rightarrow \mathbb{R}^d \rightarrow \mathbb{R}^n$$

optimized to be close to the identity (on the support of the training distribution). One may ask for the image of the reversed composition

$$\phi \circ \psi: \mathbb{R}^d \rightarrow \mathbb{R}^n \rightarrow \mathbb{R}^d ,$$

which follows the path of adversarial learning.

In particular we are interested in measuring how far from the identity the composition $\Phi = \phi \circ \psi$ is, and whether the image of the map is closer to the support of the training data. In the second case we may say that the network has contracting properties. Since the RPDs provide a natural “calibration” of the distance, we can sample vertices of an RPD at random (which are all of scaling distance 1) and observe the distribution of scaling distances of the image of Φ of those vertices.

Here, we again compare the behavior of RPDs with a standard k -means descriptor (based on sample means); see Fig. 8. We start with a sample of vertices V of a RPD for a fixed class (and hence of scaling distance to that class equal to 1) and apply map Φ to them. For comparison, we also produce the histograms for (scaled) Euclidean distances to sample mean of a class. The results of these experiments are shown in Fig. 9. Notice that while both networks exhibit a strong contractive behavior, it is especially pronounced for the VAE model. The simplest explanation for this is that the networks give a nearly constant response on the entire Voronoi cell.

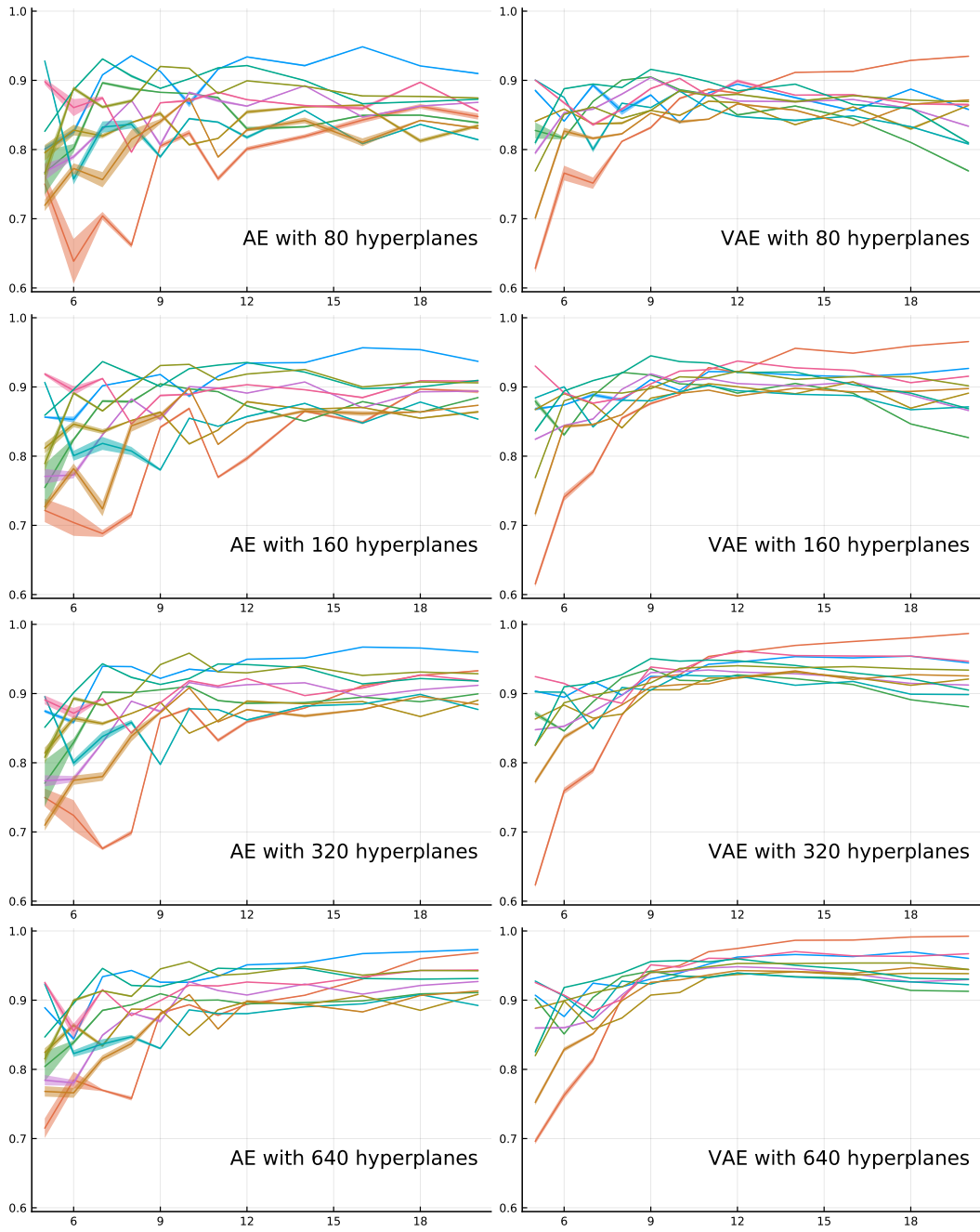


Figure 3: Results of the anomaly detection experiment on the embedded MNIST dataset. Each curve represents the performance of RPDs for one class (mean and joint variance for 5 separately trained networks and 5 RPD constructions). On the vertical axis is the AUC score; on the horizontal axis the dimensionality of embeddings.

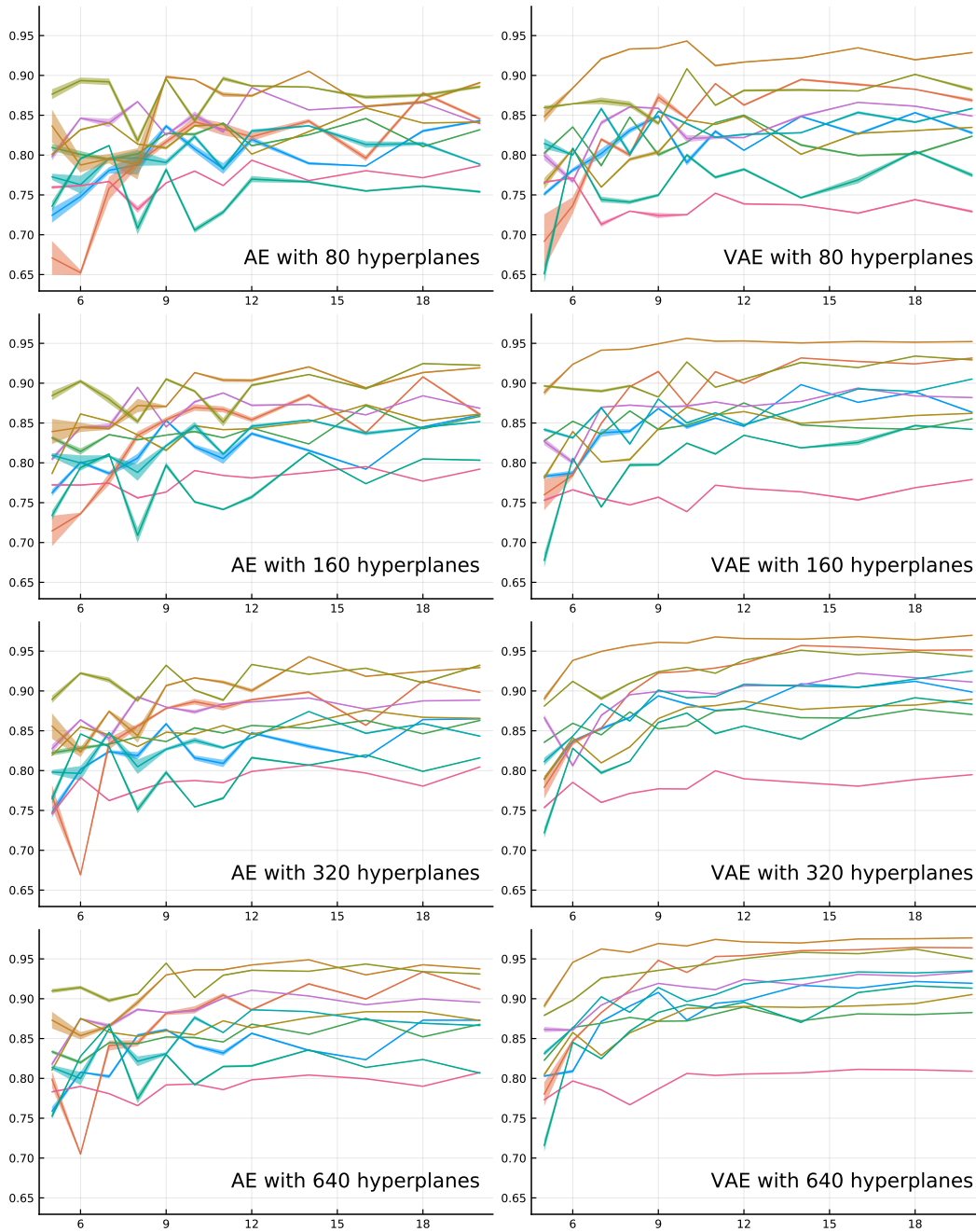


Figure 4: Results of the anomaly detection experiment on the embedded FMNIST dataset. Each curve represents the performance of RPDs for one class (mean and joint variance for 5 separately trained networks and 5 RPD constructions). On the vertical axis is the AUC score; on the horizontal axis the dimensionality of embeddings.

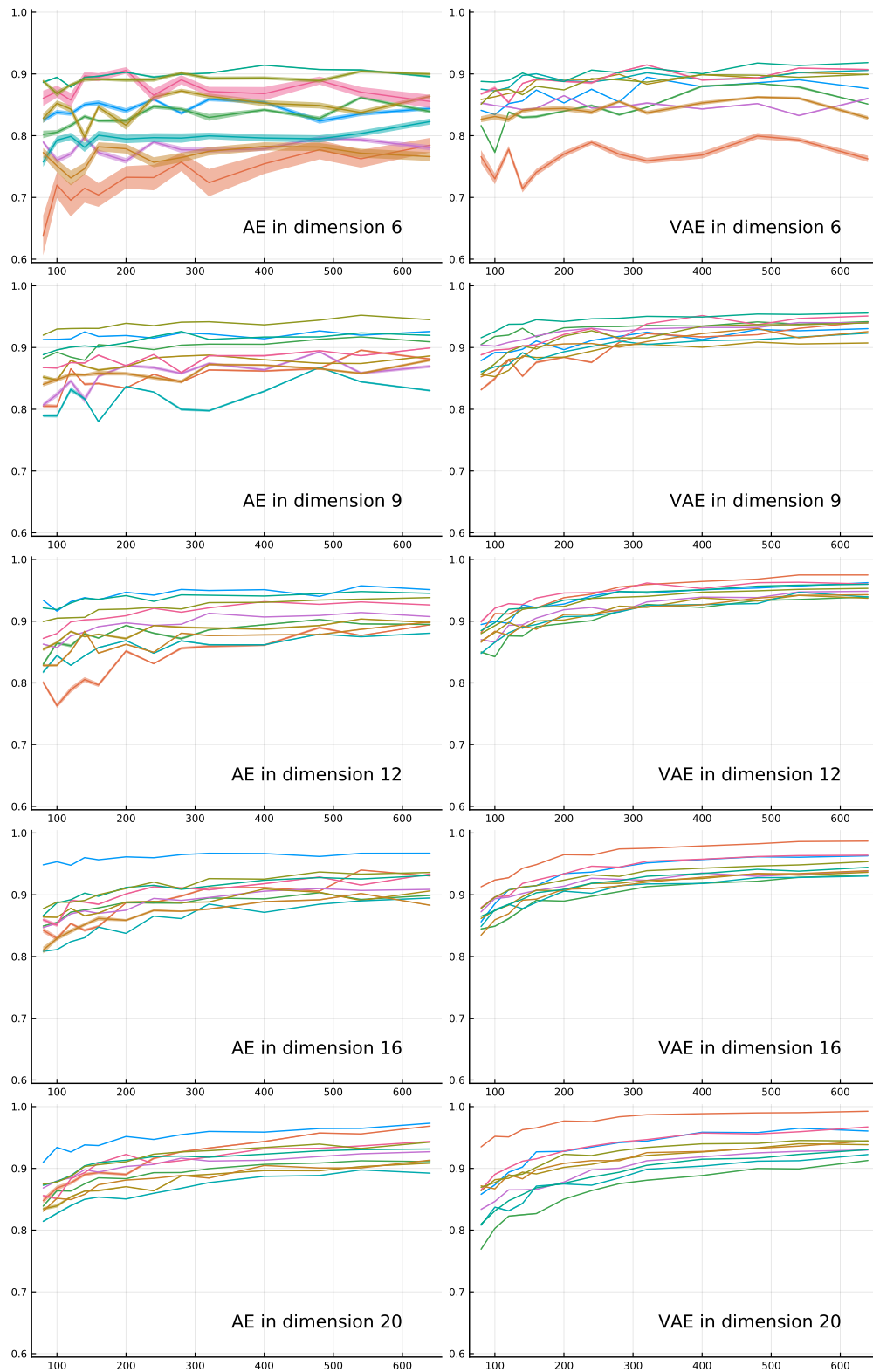


Figure 5: Results of the anomaly detection experiment on the embedded MNIST dataset. Each curve represents the performance of RPDs for one class (mean and joint variance for 5 separately trained networks and 5 RPD constructions). On the vertical axis is the AUC score; on the horizontal axis the number of hyperplanes used to define RPD.

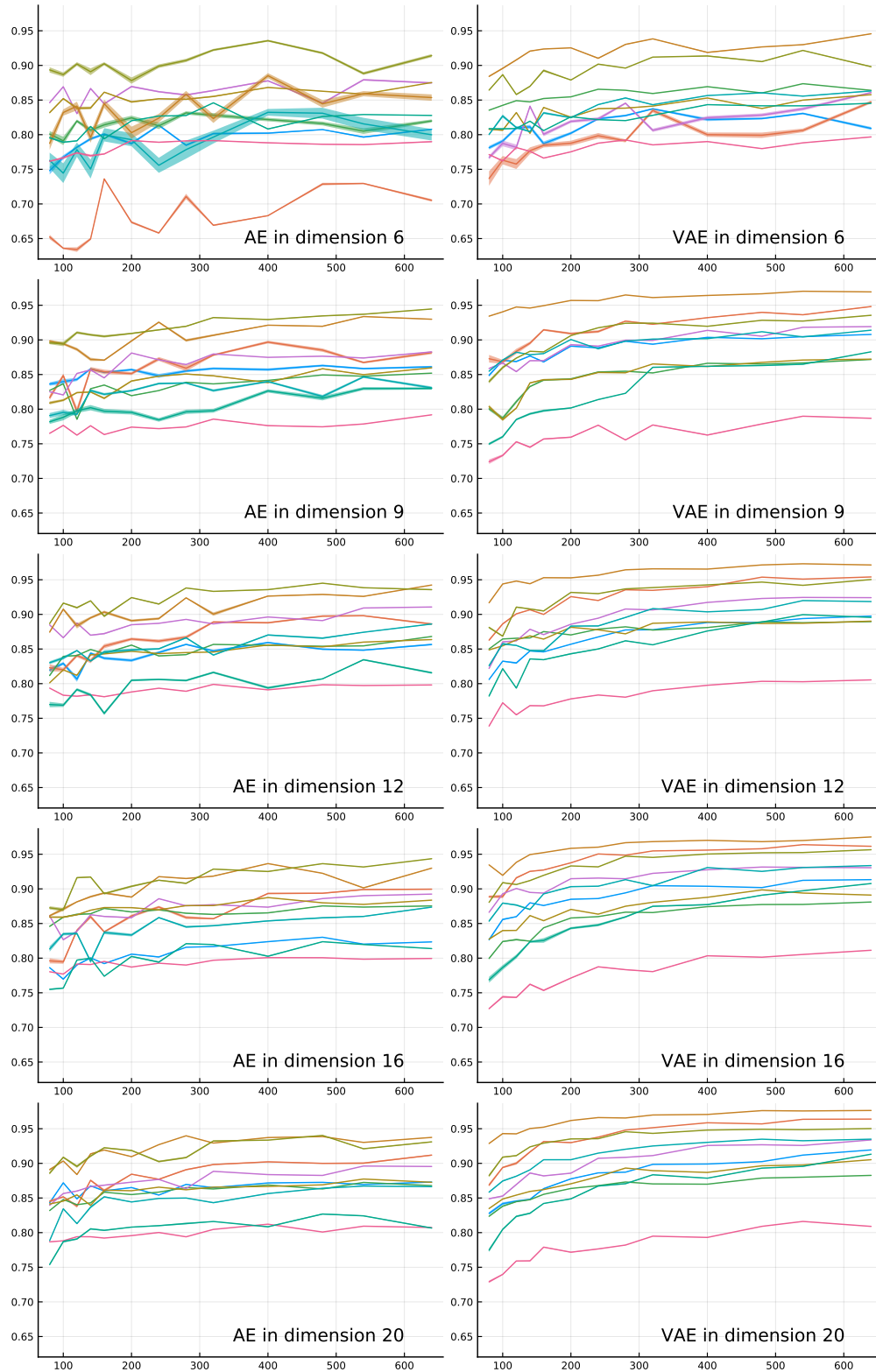


Figure 6: Results of the anomaly detection experiment on the embedded FMNIST dataset. Each curve represents the performance of RPDs for one class (mean and joint variance for 5 separately trained networks and 5 RPD constructions). On the vertical axis is the AUC score; on the horizontal axis the number of hyperplanes used to define RPD.

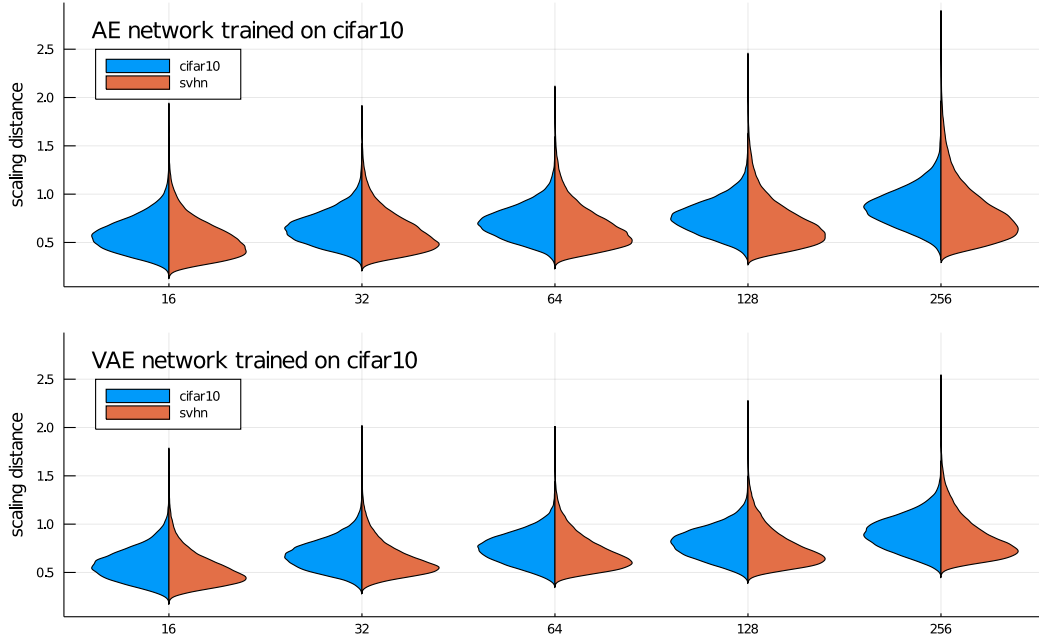


Figure 7: Results of the out-of-distribution detection experiment for CIFAR-10 (in-distribution) with SVHN (out-of-distribution) analogous to Fig. 2. We use $(m, \ell) = (40n, 1)$, where n is the dimension of the embedding. Again, five distinct AE and VAE networks were trained and independently five random polytopes were drawn for each of the dimensions.

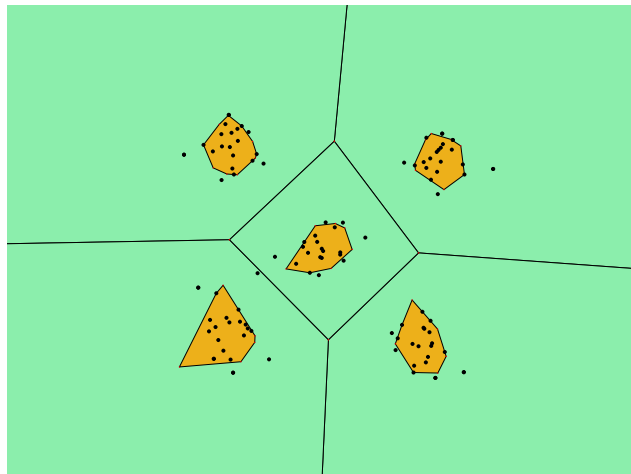


Figure 8: An illustration of our Random Polytope Descriptor (orange) vs. k -means Voronoi regions (green) on a 2D toy example ($K = 5$ classes of 20 points each; $m = 12$, $\ell = 2$). The RPD regions are bounded, whereas the Voronoi cells are unbounded. In higher dimensions the situation is considerably more intricate.

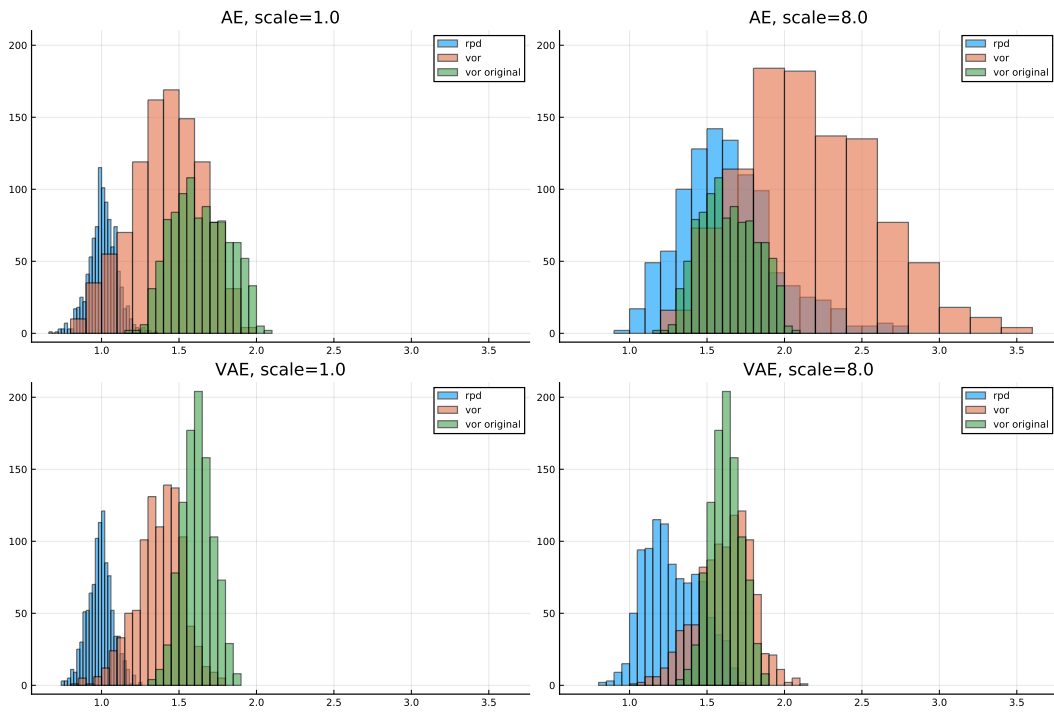


Figure 9: The distribution of scaling distance to points in $\Phi(V)$ (in blue). The sample V is of scaling distance 1 (left column) and 8 (right column). The histograms of scaled Euclidean distances to the sample mean of the class are in green (the set of vertices V) and in red ($\Phi(V)$). Notice that both networks are strongly contractive.